

## Magneto-oscillations in the high-magnetic-field state of $(\text{TMTSF})_2\text{ClO}_4$

J. S. Brooks\*

*Department of Physics, Florida State University, Tallahassee, Florida 32306*

R. G. Clark, R. H. McKenzie, R. Newbury, R. P. Starrett, and A. V. Skougarevsky

*School of Physics and National Pulsed Magnetic Field Laboratory, University of New South Wales, Sydney, 2052, Australia*

M. Tokumoto

*Electrotechnical Laboratory, Tsukuba, Ibaraki 305, Japan*

S. Takasaki, J. Yamada, and H. Anzai

*Himeji Institute of Technology, Akaho-gun, Hyogo 678-12, Japan*

S. Uji

*National Research Institute for Metals, Tsukuba, Ibaraki 305, Japan*

*and Department of Physics, Florida State University, Tallahassee, Florida 32306*

(Received 22 February 1996)

We report a systematic study of the anomalous rapid oscillation (RO) phenomena in the quasi-one-dimensional organic metal  $(\text{TMTSF})_2\text{ClO}_4$  in pulsed magnetic fields up to 51 T. We argue that the temperature and magnetic-field dependence of the RO amplitudes in the high-field state result from the reconstructed, nested Fermi surface topology at low temperatures in high magnetic fields. In this topology, the RO amplitudes depend on competing magnetic breakdown and Bragg reflection probabilities, along with Lifshitz-Kosevich reduction factors. [S0163-1829(96)01422-1]

Organic conductors based on the TMTSF [tetramethyltetraselenafulvalene] molecule are model systems in which to investigate the fundamental physics of low-dimensional electronic systems.<sup>1</sup> When slowly cooled through its anion ordering transition at 24 K,  $(\text{TMTSF})_2\text{ClO}_4$  exhibits a number of magnetic-field-dependent phases, as shown in the inset of Fig. 1. Here the magnetic field is parallel to the  $c^*$  axis, the least conducting direction. At ambient pressure  $(\text{TMTSF})_2\text{ClO}_4$  is a superconductor below 1.3 K and up to 30 mT. A cascade of phase transitions into field-induced-spin-density-wave (FISDW) phases occurs at fields above 4 T. Near 15 T the second-order FISDW transition temperature reaches a maximum of  $\approx 5.5$  K. Another phase boundary is present at  $B_{\text{RE}} \sim 28$  T, and the high-field state (HFS) above  $B_{\text{RE}}$  is also known as the reentrant phase.<sup>2</sup> Recently extensive studies of transport and magnetization have indicated that the  $B_{\text{RE}}$  line is not connected to the second-order FISDW line, and hence the HFS is not a reentrant metallic state.<sup>3</sup> Aside from the complication of the  $B_{\text{RE}}$  phase boundary, the HFS strongly represents the final  $N=0$  nested state predicted by the “standard model.”<sup>1</sup>

As a function of field *quantum oscillations*, reminiscent of de Haas-van Alphen and Shubnikov-de Haas (SdH) oscillations seen in conventional metals, are observed in transport,<sup>4-6</sup> thermodynamic,<sup>4,7,8</sup> far-infrared reflectivity,<sup>9</sup> and acoustic<sup>10</sup> properties. In Figs. 1(a) and 1(b) these oscillations are clearly seen, superimposed on the background magnetoresistance, for transport in both the  $a$ -axis and  $c^*$ -axis directions in the title material. However, since the zero-field Fermi surface is open, their origin must arise from some explanation other than quantum oscillations seen in

standard closed orbit quasi-two-dimensional metals. Although a number of theories have been proposed for the rapid oscillations<sup>11-15</sup> none are completely consistent, even qualitatively, with all the effects that are observed.

In this paper we explore the rapid oscillation (also known as “RO”) behavior in the high-field state in  $(\text{TMTSF})_2\text{ClO}_4$ . Previous pulsed-field studies by Agosta *et al.*<sup>16</sup> (see also Osada *et al.*<sup>17</sup>) have shown that the more well ordered the sample is (the  $\text{ClO}_4$  anions order at about 24 K), the greater is the ratio of the first-to-second harmonic amplitude, as seen in the Fourier transform (FT) spectrum. Although the temperature dependence of the FT amplitude of both the first ( $F_1 \approx 265$  T) and second ( $F_2 \approx 530$  T) harmonics has a maximum at about 2.1 K *within* the FISDW phases, about  $B_{\text{RE}}$  the magnetoresistance and amplitude of  $F_1$  increases with magnetic field. In the present work, we systematically investigate the temperature and field dependence of the magnetoresistance and RO amplitude *above*  $B_{\text{RE}}$  in the HFS. We find the temperature and field dependence of the oscillation amplitudes bears a strong similarity to the behavior of a system with competing magnetic breakdown and Bragg reflection probabilities, along with the Lifshitz-Kosevich (LK) reduction factors<sup>18</sup> expected for closed orbits in conventional metals.

The experiments reported here were carried out at the National Pulsed Magnet Laboratory at the University of New South Wales.<sup>19</sup> Two samples were studied in a top loading <sup>3</sup>He refrigerator. Both were aligned with the  $c^*$  axis along the magnetic field. The voltage and current were along the  $c^*$ -axis (125  $\mu\text{A}$ ) and  $a$ -axis (180  $\mu\text{A}$ ) directions for the first and second sample, respectively. The samples were cooled

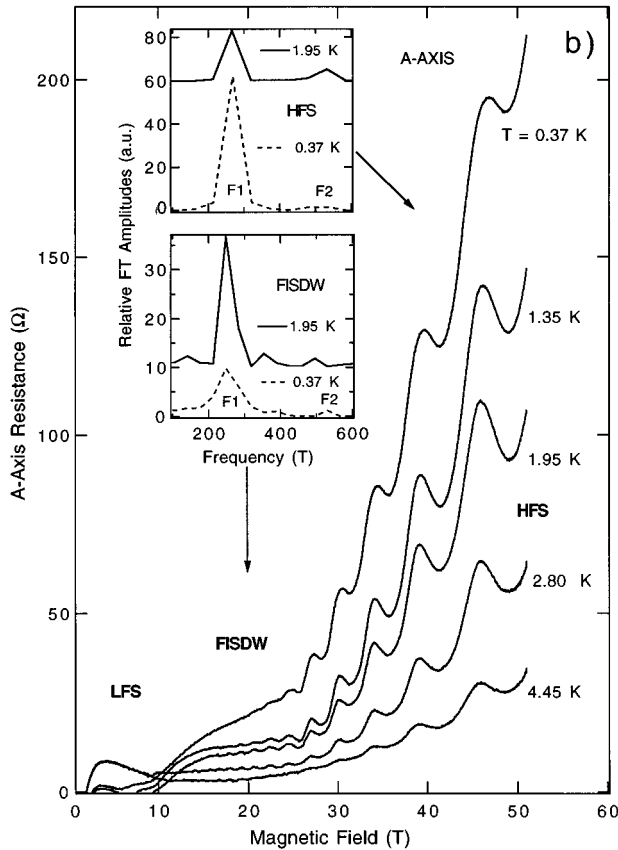
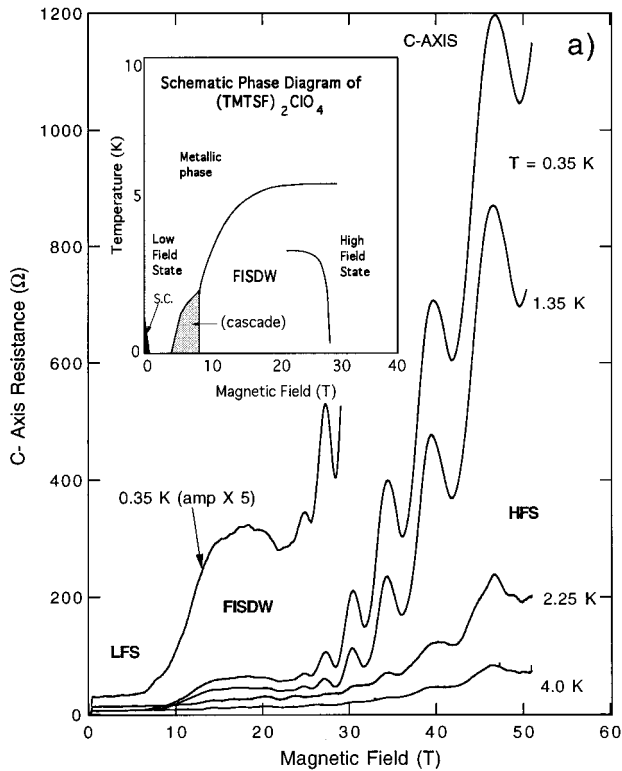


FIG. 1. Magnetoresistance and quantum oscillation behavior of  $(\text{TMTSF})_2\text{ClO}_4$  in pulsed magnetic fields. (a) Transport along the  $c^*$  axis. Inset:  $T$ - $B$  phase diagram (Ref. 3). (b) Transport along the  $a$  axis. Inset: Temperature dependent FT spectrum in FSDW and HFS regions of the phase diagram. Note the different temperature dependence of the  $F1$  amplitude in the two phases, and the relatively small  $F2$  amplitude compared with that of  $F1$ .

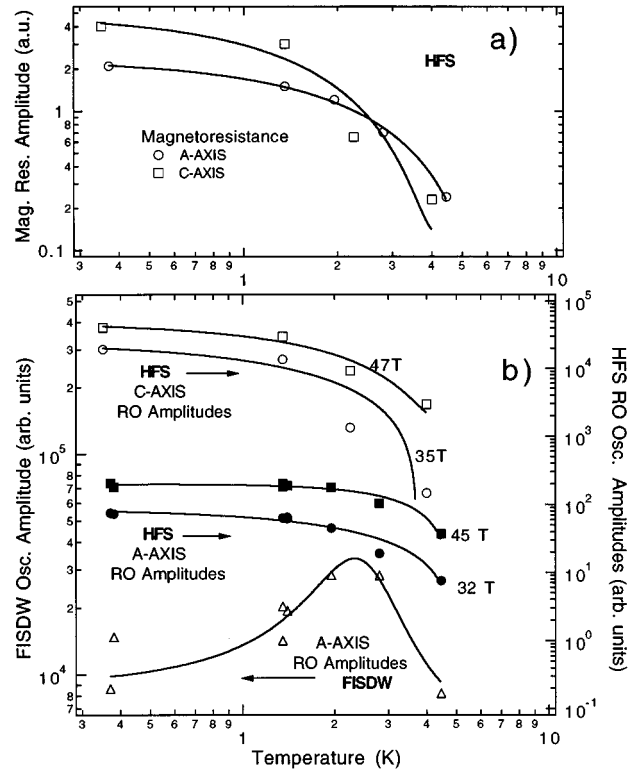


FIG. 2. (a) Temperature dependence of HFS magnetoresistance (prefactor  $R_0$  of quadratic field dependent term) for  $a$ - and  $c^*$ -axis transport. (b) Temperature dependence of the RO amplitude envelopes at low and high fields within the HFS for both  $a$ - and  $c^*$ -axis data. Also shown is the  $a$ -axis RO amplitude within the FSDW phase (determined by FT) which exhibits the well established maximum near 2.1 K. In all cases solid lines are guides to the eye.

by first loading from room temperature into the  $^3\text{He}$  system at 4.2 K. The system was then allowed to warm and remain at 20 K (just below the anion ordering temperature) for periods of up to 48 h. Test field shots taken periodically showed that the samples became very well ordered after several days. The magnet system was pulsed up to 51 T with a duration of 20 ms. Measurements were made with dc constant current sources and low noise, differential preamplifiers. Pickup from the  $dB/dt$  term was never more than 50% of the signal above 25 T. The pickup term was eliminated from the data in two ways. In some cases forward, reverse, and zero current traces were taken to subtract out and to observe directly the  $dB/dt$  term. This term scaled directly with the  $dB/dt$  term obtained from the pickup coil used to monitor the field. Hence in cases where time did not permit forward and reverse sequences, a scaled  $dB/dt$  term was used to correct the raw data. Both methods applied to the same data agree within 10% at high fields. The  $c^*$ -axis transport data, due to the parallel configuration of the leads and field, gave a superior cancellation of pickup signal at low fields where the  $dB/dt$  term was the greatest, whereas the pickup signal was more apparent in the  $a$ -axis data at low fields. A  $\text{RuO}_2$  thermometer mounted within 5 mm of the sample was used to monitor the temperature before and after each pulse. No systematic changes in temperature were observed as a result of the pulse. Possible heating effects of the

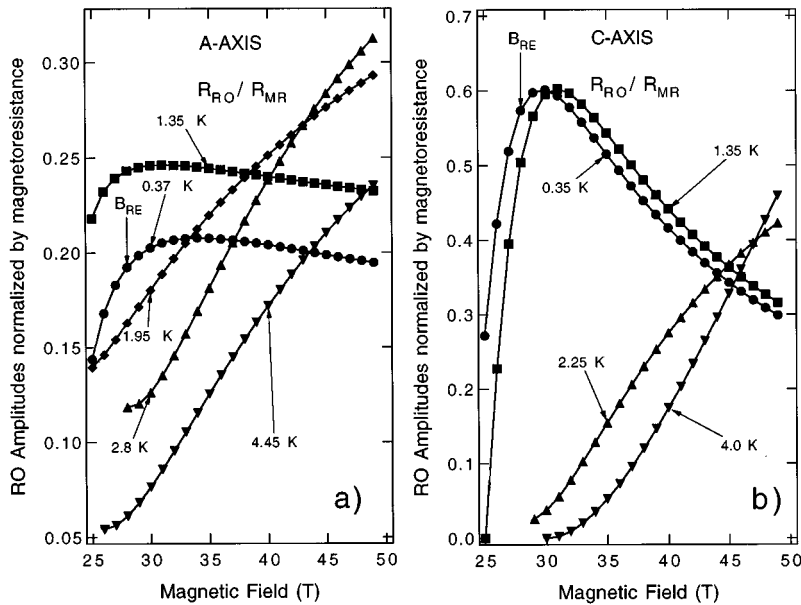


FIG. 3. Magnetic-field dependence of the RO amplitude envelopes normalized by the quadratic background magnetoresistance for the data in Fig. 1. The rapid rise in the signal at low fields and low temperatures is due to the crossing of the  $B_{RE}$  phase boundary.

sample during the pulse were checked by doubling the current. For the worst case—the  $c^*$ -axis measurements where the magnetoresistance is the largest and the current path is the shortest—we observed no systematic difference in the resistance signal within the uncertainty of the measurements (10%) at 0.37 K. Likewise, when the sample was warmed to 1.35 K, the temperature dependence of the signal faithfully followed the trends shown in Fig. 1. Power dissipation in the  $a$ -axis data was three times less, and the current path was the longest. Since both configurations yield the same results, Joule heating did not play a critical role in the measurements.

In Figs. 1(a) and 1(b) the field dependence of the resistance for  $c^*$ -axis and  $a$ -axis current orientations, respectively, are shown at several temperatures. The peak index versus inverse field is linear, and we note that the sixth quantum level is reached by 47 T. The inset in Fig. 1(b) shows the FT spectrum in the FISDW and HFS phases, indicating different temperature dependence in these two phases. In the HFS, the rapid oscillation amplitude increases monotonically with decreasing temperature. In contrast [see Fig. 2(b)], *within* the FISDW state the oscillation amplitude has a maximum at 2.1 K, consistent with previous work.<sup>16,17,20</sup> The fundamental frequency  $F1$  observed in both samples was 265 T—an indication that the  $c^*$  axes in both cases were well aligned with respect to the magnetic field.<sup>20</sup>

Temperature dependence of the magnetoresistance and RO amplitudes are shown in Fig. 2. The background magnetoresistance for both the  $c^*$ - and  $a$ -axis data was parametrized with a quadratic function of the form  $R_{bg} = \text{const.} + R_0(B - B_0)^2$ , which provided an excellent fit to the results. (We note that the offset field factor  $B_0$  was in the range of 22 to 25 T, as can be seen by inspection of the data in Fig. 1.) The temperature dependence of the quadratic prefactor  $R_0$  is shown in Fig. 2(a) for both  $a$ - and  $c^*$ -axis data. There is no evidence in our data for activated behavior in  $R_{bg}$ .

The RO amplitude was determined from the difference (envelope) of second-order polynomial fits to the peaks and valleys of the wave forms. This method of extracting the

oscillatory component of the magnetoresistance, which yields both field and temperature dependent information, is consistent with FT and individual peak-to-valley methods. The resulting amplitudes for the HFS quantum oscillations at low and high fields within the HFS are shown as a function of temperature in Fig. 2(b). Again, no activated behavior of the RO amplitudes was observed.

The main results of this paper are shown in Fig. 3. Here we have plotted the RO amplitudes *divided* by the background magnetoresistance. When SdH oscillations are measured in a metal, the background magnetoresistance must be divided out prior to applying the Lifshitz-Kosevich formalism.<sup>18</sup> Hence in the present case, if the RO behavior is the result of (effectively) closed orbit motion, then this must also be the case. We find that at high temperatures, the RO reduced amplitudes grow monotonically with field, but at low temperatures the RO reduced amplitudes actually *decrease* in the high-field limit. We note that near  $B_{RE}$  the reduced RO amplitudes appear to increase rapidly since they attenuated within the FISDW state, and appear to suddenly “grow” as the HFS is entered. This is most evident in the very low-temperature data. Due to the superior signal-to-noise in the  $c^*$ -axis data (less pick-up and higher sample resistance), the temperature and field dependence of the reduced RO amplitudes in Fig. 3(b) best describe the behavior. The relative variation in the absolute values of the reduced RO amplitudes (which are  $\approx 1/2$  the  $c^*$ -axis values) are most likely the result of experimental and analytical uncertainties.

The temperature and field dependence of the magnetoresistance and quantum oscillations above the phase boundary at 28 T, and below 5.5 K (i.e., in the HFS) are best described as follows. *First*, the quantum oscillation amplitude (before division by the magnetoresistance) is at best weakly quadratic, if not linear, with magnetic field, and the temperature dependence is not activated. *Second*, the magnetoresistance is quadratic in field, and its amplitude increases with decreasing temperature, but not in an activated manner. To address the origin of the observed behavior of the RO in the HFS, we consider the evolution of the Fermi surface (FS)

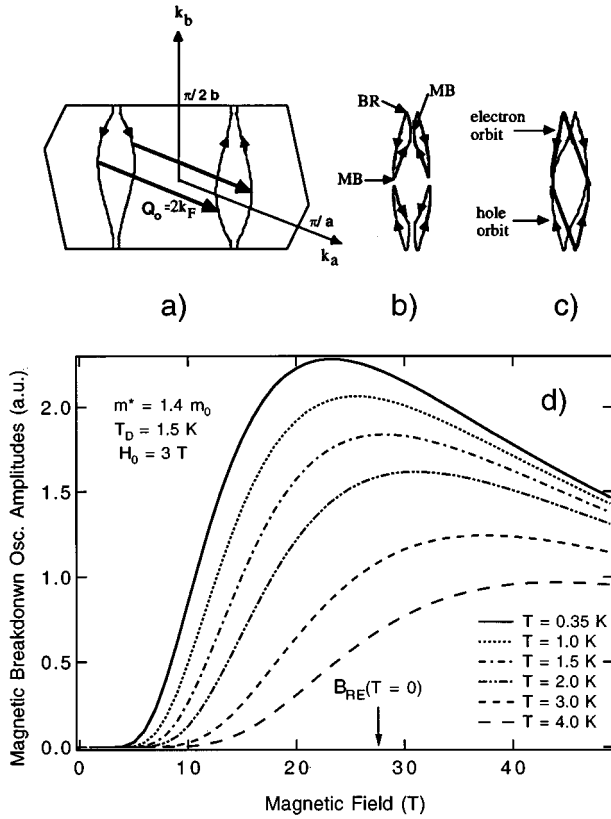


FIG. 4. Consequences of Fermi surface reconstruction and nesting in  $(\text{TMTSF})_2\text{ClO}_4$ . (a) Reconstructed FS based on original band-structure calculations (Ref. 22). The final nesting vector is indicated. (The  $b$ -axis dispersion  $t_b$  has been exaggerated by a factor of about 3 to reveal details.) (b) Resulting field-dependent closed orbit pockets, with magnetic breakdown (MB) and Bragg reflection (BR) points indicated. (c) Electron and hole orbits which result from the lowest order MB and BR processes. Arrows in all cases refer to trajectories for magnetic field applied out of the paper. (d) Predicted RO amplitude behavior based on the MB/BR model. In the high-field limit, the amplitude must vanish since the BR probability goes to zero. Note that the model is only applicable above the (temperature-dependent)  $B_{\text{RE}}$  field.

with temperature and magnetic field, as is shown in Figs. 4(a)–4(c). At the anion ordering temperature the original quasi-one-dimensional FS reconstructs due to the doubling of the unit cell along the  $b$  axis. This topology alone can give rise to Stark interference orbits in the metallic (LFS) state, the field and temperature dependence of which has been recently treated by Uji *et al.*<sup>20</sup> In sufficiently high magnetic fields, this reconstructed FS nests with a quantized, magnetic-field-dependent nesting vector  $Q_N = 2k_F + N(\text{beH}/\hbar)$ , as described by the “standard model.” (Here  $N = 0, 1, 2, 3$ , etc.) The nesting is imperfect, and small pockets remain, giving rise to a quasi-SdH oscillation frequency (since the nesting vector is field dependent). In the high-field limit, the standard model predicts a final nesting vector  $N = 0$ , i.e.,  $Q_0 = 2k_F$  as shown in Fig. 4(a).

Figures 4(b) and 4(c) serve as the basis for comparison with our results. We first address the behavior of the RO amplitudes. We note that a very similar topologies have recently been considered by Kishigi and Machida<sup>21</sup> and by McKernan *et al.*<sup>3</sup> In the former case  $Q_0$  was considered, but in the latter case two different nesting vectors were used to explain the data in the vicinity of the  $B_{\text{RE}}$  phase boundary. In our estimation  $Q_0$  is more physical (based on the topology), at least in very high fields. In Figs. 4(b) and 4(c), there are several mechanisms which control the motion of carriers on the Fermi surface. First, the area of the very small, closed orbit pockets, represent a frequency of 35 T.<sup>4</sup> Hence even if these pockets remain, they are in the quantum limit in the HFS, and cannot contribute directly to the RO behavior. Secondly, because of the topology of the nested/reconstructed FS, magnetic breakdown and Bragg reflection can occur at the points indicated in Fig. 4(b), thereby producing the larger frequency orbits shown. The magnetic breakdown probability at any one vertex is  $P_{\text{MB}} = \exp(-H_0/H)$  where we take  $H_0 = 3$  T,<sup>20</sup> and for the Bragg points is  $P_{\text{BR}} = 1 - \exp(-H_0/H)$ . The appropriate LK reduction factors are the Dingle term  $R_D = \exp(-14.7T_D m^*/m_0 H)$  and the temperature term  $R_T = (14.7m^* T/m_0 H)/\sinh(14.7m^* T/m_0 H)$ . For the sake of definiteness, we have taken the Dingle temperature  $T_D$  to be 1.5 K and  $m^*$  to be  $1.4 m_0$ . Hence the temperature and field dependence of the amplitudes of the resulting electron and hole orbits, each of which involves four breakdown and two Bragg points is proportional to  $P_{\text{MB}}^4 P_{\text{BR}}^2 R_D R_T$  as is shown in Fig. 4(d). Of note in Fig. 4(d) is that at fields of order 30 T, the RO amplitudes increase with field at high temperature, but actually decrease with field at low temperature. Although there are some uncertainties in the RO amplitude data in Fig. 3, both  $a$ - and  $c^*$ -axis data exhibit the same basic behavior. Hence the above breakdown/reflection model provides the essential features needed to describe the RO mechanism in the HFS.

Finally, we turn to the temperature and field dependence of the background magnetoresistance in the HFS. The form of the magnetoresistance expected for a compensated closed orbit system is  $R_{bg} \approx R_0(1 + \omega_c^2 \tau^2)$ . Here the residual resistivity goes as  $R_0 = m^*/ne^2 \tau$ . Hence  $R_{bg}$  should be quadratic in field, and since  $\tau$  and therefore  $R_0$  saturate at low temperatures, so should the temperature dependence of  $R_{bg}$ . This is exactly what is observed.

In conclusion, by following the basic principles of FS reconstruction, the “standard model” for nesting, and a straightforward application of a semiclassical model for magnetic breakdown and Bragg reflection, we can capture the essential features of the RO behavior in the HFS of  $(\text{TMTSF})_2\text{ClO}_4$ . We further note that recent Hall-effect data<sup>23</sup> indicates that the Hall sign oscillates about zero in the HFS. This may be a result of the oscillation in the nearly perfect electron/hole compensation which is a property of the FS in Fig. 4(c).

This work was supported by the Australian Research Council and NSF DMR 92-14889 and 95-10427.

\*Electronic address: brooks@magnet.fsu.edu.

- <sup>1</sup>For a review, T. Ishiguro and K. Yamaji, *Organic Superconductors* (Springer-Verlag, Berlin, 1990).
- <sup>2</sup>M. J. Naughton *et al.*, Phys. Rev. Lett. **61**, 621 (1988).
- <sup>3</sup>S. K. McKernan *et al.*, Phys. Rev. Lett. **75**, 1630 (1995).
- <sup>4</sup>X. Yan *et al.*, Phys. Rev. B **36**, 1799 (1987).
- <sup>5</sup>J. P. Ulmet *et al.*, Solid State Commun. **58**, 253 (1986).
- <sup>6</sup>A. Audouard *et al.*, Phys. Rev. B **50**, 12 726 (1994), and references therein.
- <sup>7</sup>N. A. Fortune *et al.*, Phys. Rev. Lett. **64**, 2054 (1990).
- <sup>8</sup>R. C. Yu *et al.*, Phys. Rev. Lett. **65**, 2458 (1990).
- <sup>9</sup>A. S. Perel *et al.*, Phys. Rev. Lett. **67**, 2072 (1991).
- <sup>10</sup>X. D. Shi, W. Kang, and P. M. Chaikin, Phys. Rev. B **50**, 1984 (1994).
- <sup>11</sup>A. G. Lebed' and P. Bak, Phys. Rev. B **40**, 11 433 (1989).
- <sup>12</sup>T. Osada, S. Kagoshima, and N. Miura, Phys. Rev. Lett. **69**, 1117 (1992).
- <sup>13</sup>Y. M. Yakovenko, Phys. Rev. Lett. **68**, 3607 (1992).
- <sup>14</sup>K. Maki, Phys. Rev. B **49**, 12 362 (1994).
- <sup>15</sup>A. G. Lebed', Phys. Rev. Lett. **74**, 4903 (1995).
- <sup>16</sup>C. C. Agosta *et al.*, in *High Magnetic Fields in the Physics of Semiconductors*, edited by D. Heiman (World Scientific, Singapore, 1995), p. 738.
- <sup>17</sup>T. Osada *et al.*, Solid State Commun. **60**, 441 (1986).
- <sup>18</sup>D. Shoenberg, *Magnetic Oscillations in Metals* (Cambridge University Press, Cambridge, 1984).
- <sup>19</sup>For a description see R. G. Clark *et al.*, Physica B **201**, 565 (1994).
- <sup>20</sup>S. Uji *et al.*, preceding paper, Phys. Rev. B **53**, 14 399 (1996).
- <sup>21</sup>K. Kishigi and K. Machida, Phys. Rev. B **53**, 5461 (1996).
- <sup>22</sup>P. M. Grant, Phys. Rev. B **27**, 3934 (1983).
- <sup>23</sup>P. M. Chaikin (private communication).